An Efficient Algorithm for Radiowave Coverage Prediction in Urban Microcells

Daniela N. Schettino, Daniel H. D. Carvalho and Fernando J. S. Moreira
Universidade Federal de Minas Gerais, Belo Horizonte MG, Brazil

Abstract— **This work presents an algorithm to perform radiowave coverage predictions in urban environments using the Uniform Theory of Diffraction (UTD). The ray-tracing algorithm is based on the image theory for a *quasi*-3D environment. Multiple reflections and diffractions are considered through the separation of multipath components into four different classes, used to determine the scattered field. The use of such classes eliminates redundant calculations throughout the ray-tracing process, improving the characterization of the power distribution over the coverage area.**

Keywords— **Radio channel characterization, radiowave propagation, uniform theory of diffraction, ray tracing.**

I. Introduction

The growing demand for mobile communications, specially in urban areas, leads toward the adoption of the microcellular concept. It is then desirable to perform accurate coverage predictions upon such microcells in order to minimize on-site measurements. Statistical prediction models can show considerable error, making necessary the adoption of more precise techniques, such as deterministic techniques. Some techniques have been proposed in the last decades and those based on ray tracing and the uniform theory of diffraction (UTD) seem to be the most efficient for the problems at hand [1]–[5]. The UTD is an asymptotic technique, based on ray tracing, that can account for multipath components between the transmitter and the receiver [6].

The first step in the evaluation of the scattered field based on the UTD is the determination of the optical paths (ray paths) between transmitter and receivers. Basically, there are two approaches for tracing such rays throughout the radio channel: the image theory (IT) [1],[2] and the shooting-and-bouncing ray (SBR) technique [3]. The IT is more rigorous than the SBR as the former is capable of determining all ray-path components–including diffracted rays–without redundancies. The IT uses optical images of the transmitter and diffraction points, considering the surfaces as reflectors. In the present work, only the direct, reflected and diffracted ray-path components are considered, with a maximum number of N_R reflections and N_D diffractions. The UTD is then used to asymptotically evaluate the electromagnetic field associated with each ray.

Daniela N. Schettino, Daniel H. D. Carvalho and Fernando J. S. Moreira, Federal University of Minas Gerais, Dept. Electronic Engineering, Av. Pres. Antonio Carlos 6627, Pampulha, Caixa Postal 209, 30161-970 Belo Horizonte, MG, Brazil, Tel. (+5531) 3499-4861, FAX (+5531) 3499-4850, fernando@eee.ufmg.br.

In order to predict the power distribution over a certain urban region, observers (receivers) are placed over the area of interest. The ray tracing and the asymptotic evaluation of the scattered field are then determined for each observer. So, the calculation of the multipath components that reach each observer can be a very time consuming process. The main objective of the present work is to present a technique where multiple reflections and diffractions are considered in the calculation of the scattered field through the separation of the ray paths into four different classes: transmitter-receiver ($T-R$), transmitter-diffraction point ($T-D$), diffraction point-diffraction point ($D-D$), and diffraction point-receiver ($D-R$). The attainment of such classes is a uniform process, as only reflections are considered inside each different class. The complete ray paths between transmitter and receiver, accounting for multiple reflections and diffractions, are then formed by the judicious concatenation of these classes, allowing a single calculation and storage for rays appearing in several distinct paths. The procedures for the formation and use of these classes are described in Sect. II. In Sect. III a case study will be presented, illustrating the the advantages of using the above mentioned classes in the ray tracing algorithm.

II. Ray Tracing Algorithm

In this section the techniques used to perform the ray tracing in a 2D environment will be presented. First, we will present the techniques adopted in the determination of the multiple reflections, based on the image theory (IT). Then, the inclusion of the diffracted rays into the ray-tracing technique will be described. Furthermore, the formation of the complete ray paths between the transmitter and the receiver, with multiple reflections and diffractions, will be considered by the definition of four different ray classes: $T-R$, $T-D$, $D-D$, and $D-R$. At last, it is discussed the conversion of the two-dimensional (2D) paths into three-dimensional (3D) paths, to be applied into the *quasi*-3D model [5].

The environment of the urban radio channel will be described by an approximate model. This simplification is based on a two-dimensional (2D) representation of the scenario, where the environment's obstacles (e.g., buildings) are represented by infinite cylinders with arbitrary cross section and vertical wedges, parallel to each other. Such

obstacles are then represented through an horizontal cut, describing the obstacle's cross sections, as illustrated in Fig. 1.

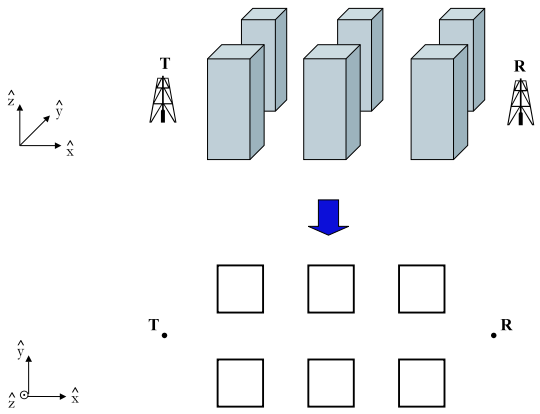

Fig. 1. 2D representation of the urban radio channel: horizontal view.

A. *Reflected Rays*

The IT is used to determine the reflected ray paths [1],[2]. In this technique, the transmitter (T) is successively reflected by the planar faces of the many obstacles, in order to find all the optical paths toward the receiver (R). This means that the IT calculates the transmitter's images from the facets that form the obstacles, represented as segments ($\overline{S}$) in the 2D model. Then, each one of these images goes through the same process, i.e., the images determined in the preceding iteration are used as (virtual) sources in the present iteration, forming a set of second order images. This process is successively repeated until a pre-determined number of image levels is attained, where such number is given by the maximum number of reflections (N_R) to be considered [1],[2].

The successive images of T are organized in an hierarchical fashion tree, where the tree's root is the transmitter (T), as illustrated in Fig. 2. The next level of the tree contains the first-order images of T, generated by the many obstacle facets. The second level contains the second order images (i.e., the images of the first order images), and so on. The indices (i,j,k,...) represent the facets (segments $\overline{S}_i$,$\overline{S}_j$,$\overline{S}_k$,..., in the 2D model) that generate such images. Note that adjacent indices are never identical, since the facet that generates a certain image can not generate its next level image. Finally, note from Fig. 2 that each image is directly connected to its (virtual) source, such that any relevant information (such as the facet where reflection occurred) can be easily retrieved.

It is worthwhile to mention that, throughout the process, several images do not need to be considered and, consequently, stored in the tree. First of all, since not all the facets $\overline{S}$ are reflectors to the (virtual) source, many of them will not contribute to the image's tree and can be immediately

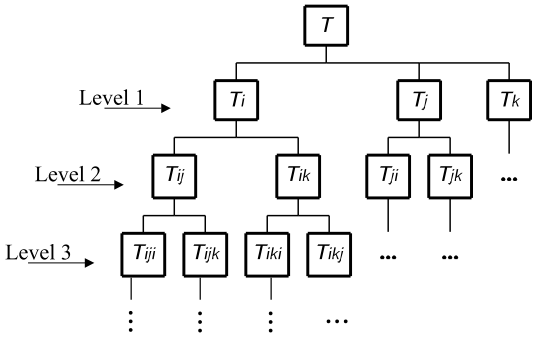

Fig. 2. Image Tree.

discarded. If this is not the case, there are still two possibilities that can preclude the image formation and, if detected *a priori*, applied toward the saving of memory space used to store the tree. One is based on the fact that only the facets partially or totally contained within the Lit Region of the (virtual) source can contribute to the formation of the next-level images [1],[2]. Besides, the contribution will occur only if such facet is not totally obstructed by another facet in the Lit Region. Such acceleration techniques make the ray-tracing procedure very efficient, mostly for those scenarios where many obstacles are present [5].

After determining all the necessary images, the next step is to identify the reflection points over the corresponding facets. To illustrate this process, consider Fig. 3, that illustrates the definition of a doubly reflected ray path. First, the receiver R is connected to the second order image T_{ij} (which is the image of T_i through $\overline{S}_j$), forming a segment that must intercept $\overline{S}_j$ in order to describe a valid reflection. If such intersection occurs, it determines the location of the second reflection point (Q_2), as illustrated by Fig. 3. If not, such doubly reflected ray path is not practical and the process is started for a different path. To locate the point where the first reflection occurs (Q_1), the point Q_2 is now connected to the first order image T_i. This new segment must intercept the segment ($\overline{S}_i$) that originates T_i, for the first reflection to be a valid one. This intersection then locates Q_1. So, the doubly reflected ray path of the present example is identified by the following points: $T \rightarrow Q_1 \rightarrow Q_2 \rightarrow R$ (Fig. 3). If Q_1 or Q_2 is not within the respective segment ($\overline{S}_i$ and $\overline{S}_j$, respectively), this ray path is disregarded and the process continues with the investigation of a different path. Finally, for the ray path to be considered a valid one, the segments $\overline{TQ_1}$, $\overline{Q_1Q_2}$ and $\overline{Q_2R}$ of the present example must not be obstructed by other segments $\overline{S}_k$ representing the obstacles' facets. The obstruction test can be efficiently implemented by some acceleration techniques, as the Space Volumetric Partition (SVP) [4].

The procedure used to identify the reflection points is performed for all the images stored in the tree. The images of the first level (see Fig. 2) can generate singly reflected ray

paths, the second-level ones can generate doubly reflected paths, and so forth. Consequently, in order to trace rays with a maximum number of N_R reflections, images up to the N_R-th level must be considered *a priori*. Finally, note that the very same procedure, described above, can be used for those cases where the observer is a diffraction point (D) instead of the receiver (R). This means that the procedure is used either for the $T-R$ class or the $T-D$ class.

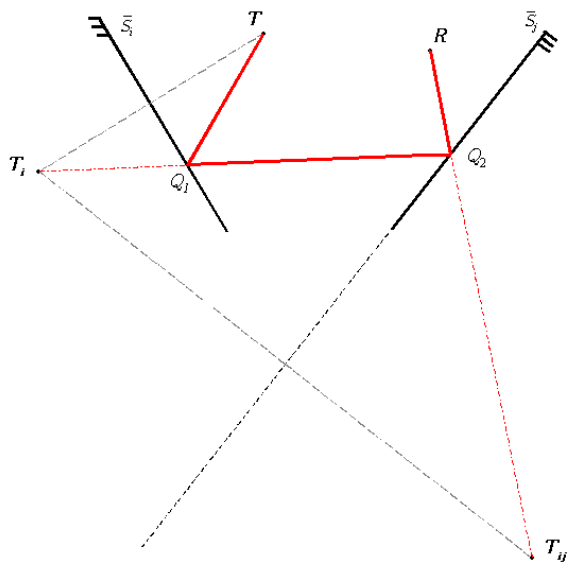

Fig. 3. Reflection points identification, using the Image Method.

B. Diffracted Rays

The inclusion of the diffraction effects is extremely important, specially for those regions with severe blockage mechanisms [2]–[4]. In order to determine the diffracted ray-paths, first we need to locate the associated diffraction points located over the obstacles' wedges. As a two dimensional description of the urban environment was adopted, such wedges are reduced into points, which describe the junctions between consecutive segments $\overline{S}$ representing the obstacles' facets.

After locating the diffraction points D (i.e., after identifying the wedge locations), each one of them will be dealt as a transmitting source. Consequently, image trees are constructed for each one of these sources, exactly as described in Sect. II-A for T. The main difference is that now adjacent segments, associated with the diffraction wedge, do not form first-level images of the corresponding D.

So, to determine the image tree of a diffraction point D, first we determine which facets are within the visibility region of this diffraction point, similarly to the Lit Region test described in Sect. II-A [1],[2]. This visibility region is delimited by the facets that form the diffraction wedge. Of the facets within this region, only those with the reflector face turned to the diffraction point are considered. The high-level images are then determined following the very same procedure described in Sect. II-A. The possible obstructions of the ray paths by the several facets are also considered with the help of the SVP technique [4].

So, the images contained in the several levels of the tree associated with a diffraction point D are used to trace rays leaving this point, passing through many (or none) reflections, and arriving at a receiver R (for those paths of a $D-R$ class) or at a diffraction point D ($D-D$ class). It is worthwhile to mention that once the paths between two diffraction points D_i and D_j are determined, the paths between D_j and D_i are directly obtained by reversing the orientation of the previous paths. Also, note that D_i and D_j can describe the very same diffraction point, where, in this case, at least one reflection must exist between then.

C. Ray Classes

The procedure to determine the multipaths between T and R, considering multiple reflections and diffractions, starts by the construction of the four different classes ($T-R$, $T-D$, $D-D$, and $D-R$), as described in Sects. II-A and II-B, where only multiple (or none) reflections are considered in each class. After the determination of the ray paths in each class, many links are done among these classes in order to obtain the multipaths between T and R passing through several reflection and diffraction points, until a maximum of N_R reflections and N_D diffractions are attained.

The ray paths between T and R that do not suffer any diffraction are directly obtained from the rays stored in the $T-R$ class. To determine ray paths passing through a single diffraction point, first it is necessary to pick up a path leaving the transmitting antenna (T) and arriving at a diffraction point (D_i) inside the $T-D$ class. Then, a path leaving D_i and reaching R is chosen from the $D-R$ class. If more than one diffraction is to be considered, the procedure is quite similar. In this case, paths from the $D-D$ class must be included between the elements of the $T-D$ and the $D-R$ classes. For example, in order to obtain a ray path with two diffractions, one element of the $D-D$ class is linked with corresponding rays of the $T-D$ and $D-R$ classes. In a similar way, to obtain a ray path with three diffractions, we start with an element of the $T-D$ class, link it with two corresponding elements of the $D-D$ class, consecutively, and, finally, a path from the $D-R$ class is linked with the last $D-D$ path. Obviously, all such links assume that the linking point D between consecutive classes is the same. Figure 4 illustrates a case where a ray belonging to the $T-D$ class and another belonging to the $D-D$ class are reused in the description of two different ray paths for two different receivers.

Once all the possible combinations among the classes' elements are made (i.e., the multipaths between T and R are traced), the procedure to trace two-dimensional rays is

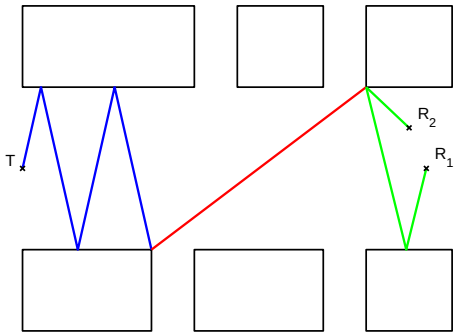

Fig. 4. Ray paths for two different receivers, with rays belonging in common to the $T-D$ and $D-D$ classes.

concluded. To complete the ray tracing process, it's still necessary to convert the 2D ray paths into 3D ones, which is discussed in the next section.

D. Conversion of 2D Ray Paths into 3D Ones

In the present work a *quasi*-3D representation for the environment is adopted [5]. In this model, the antennas heights are assumed much smaller than the obstacles heights, so diffractions and reflections on the top wedges and facets have minor effects and, consequently, are neglected. The ground is assumed planar, so that the vertical wedges' edges are all perpendicular to the ground plane and, consequently, parallel to each other. In this scenario, the *quasi*-3D model consider ground reflection by simply applying the image concept to the receiver (or transmitter) with respect to the ground plane [5]. Consequently, each optical path between T and R, independently from the number of reflections and diffractions over the several obstacles, will have a counterpart that leaves T and reaches the image of R; the later is never reflected by the ground, while the former describes a path reflected once by the ground. Consequently, due to the assumed geometry, both paths will have the very same projection in the ground plane, which corresponds to a 2D path as previously discussed. In other words, each 2D path will generate two different 3D paths for the *quasi*-3D model, one of them suffering a single reflection over the ground plane. The conversion of 2D ray paths into 3D ones is done with the help of the total distance measured along the 2D path and the antennas heights with respect to ground. This procedure is detailed in [5].

III. Case Study

In order to demonstrate the ray-tracing techniques previously discussed, a practical case study was investigated. The urban environment adopted was that of [7], which refers to a region of Ottawa, Canada, depicted in Fig. 5. This figure also indicates the transmitter and receivers locations, chosen as in [7]. The field was asymptotically evaluated by the UTD with $N_R = 5$ and $N_D = 2$. A vertically polarized Hertz dipole was used as the transmitter at 910 MHz. As suggested in [8], the relative permissivity and the conductivity of the obstacles (buildings) are 7 and 0.2 S/m, respectively, while 15 and 0.05 S/m, respectively, were adopted for the ground. The UTD results (shown in Fig. 6(a)), when compared to the measured results of [7] (shown in Fig. 6(b) together with the UTD results of [8]), present disagreements of about 10 dB at most, at very specific points.

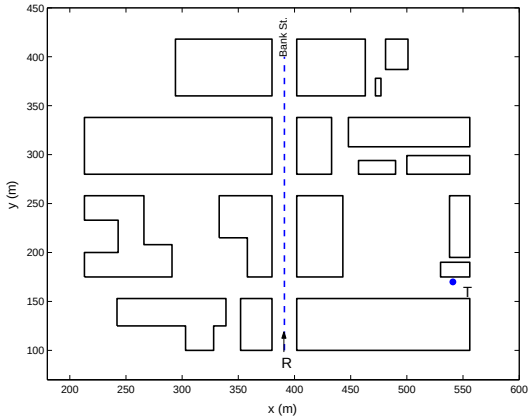

Fig. 5. Part of Ottawa city streets configuration. Observation through the Bank St.

In order to perform coverage prediction, many receivers are used to cover the region of interest, keeping the transmitter in the same position. Consequently, all the elements of the $T-D$ and $D-D$ classes just need to be determined once, improving the processing time of the ray-tracing routine. In the example of Figs. 5 and 6, 150 receivers where used (1 at each 2 meters). In the first simulation (first receiver), all the four classes were calculated. From the second receiver on, only the $D-R$ and $T-R$ classes needed to be recalculated, since the $T-D$ and $D-D$ classes ray paths have already been defined. It means that from the second receiver on, the time spent by the implemented program to calculate the path loss is 3 times lower compared to the first simulation, for each new receiver.

The determination of the multipaths through the use of these ray classes makes possible that many elements of a class that appear several times in different ray paths just need to be determined and stored once. It consists in another advantage in the utilization of these classes, since some rays may appear dozens of times (Fig. 4). Fig. 7 shows examples of how many times rays belonging to the $T-D$, $D-D$ and $D-R$ classes are reused (percentage of the total amount of rays used in each class), for a receiver located at (391 m, 100 m), in the configuration depicted in Fig. 5. This means that Fig. 7 shows how many times the rays are reused inside the respective class to form different ray paths reaching the specific receiver.

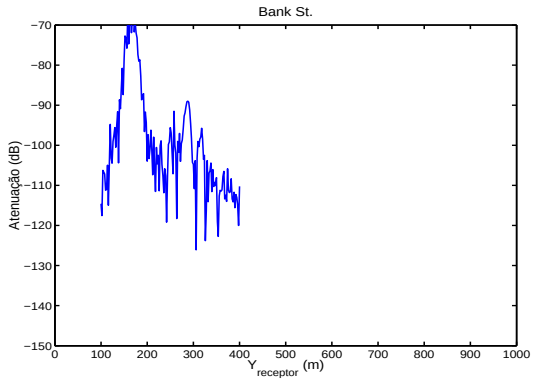

(a) UTD path loss, with receivers through the Bank St. and transmitter at (541 m, 170 m).

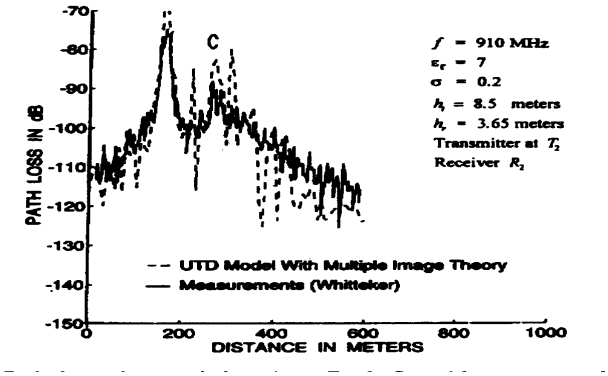

(b) Path loss through the Bank St.: measures and UTD prediction (Fig.4 of Ref. [8].

Fig. 6. Path loss through the Bank St.

IV. Conclusion

This work presented an efficient ray-tracing algorithm through the separation of the ray paths in four different classes: $T-R$, $T-D$, $D-D$ and $D-R$, improving the time spent to perform coverage prediction. With the utilization of these classes, several rays that appear in many different ray paths do not have to be recalculate. Besides, for different receivers in a coverage prediction, rays belonging to the $T-D$ and $D-D$ classes just need to be determined once. The formation of the classes is done by an uniform procedure that uses the Image Theory to determine reflection points, where some acceleration techniques are used to reduce the total processing time.

References

[1] M. C. Lawton and J. P. McGeehan, "The Application of a Deterministic Ray Launching Algorithm for the Prediction of Radio Channel Characteristics in Small-Cell Environments," *IEEE Trans. Veh. Technol.*, vol. 43, pp. 955–969, Nov. 1994.

[2] K. Rizk, J.-F. Wagen, and F. Gardiol, "Two-Dimensional Ray-Tracing Modeling for Propagation Prediction in Microcellular Environments," *IEEE Trans. Veh. Technol.*, vol. 46, pp. 508–518, May 1997.

[3] G. Liang and H. L. Bertoni, "A New Approach to 3-D Ray Tracing for Propagation Prediction in Cities," *IEEE Trans. Antennas Propagat.*, vol. 46, pp. 853–863, June 1998.

[4] M. F. Catedra and J. Perez-Arriaga, *Cell Planning for Wireless Communications*, Artech House - Mobile Communications Series, 1999.

[5] H.-W. Son and N.-H. Myung, "A Deterministic Ray Tube Method for Microcellular Wave Propagation Prediction Model," *IEEE Trans. Antennas Propagat.*, vol. 47, pp. 1344–1350, Aug. 1999.

[6] R. F. Kouyoumjian, and P. H. Pathak, "A Uniform Geometrical Theory of Diffraction for an Perfectly Conducting Surface," *Proc. IEEE*, vol. 62, pp. 1448-1461, Nov. 1974.

[7] J. H. Whitteker, "Measurements of Path Loss at 910 MHz for Proposed Microcell Urban Mobile Systems," *IEEE Trans. Veh. Technol.*, vol. 37, pp. 125–129, Aug. 1988.

[8] S. Y. Tan and H. S. Tan, "Propagation Model for Microcellular Communications Applied to Path Loss Measurements in Ottawa City Streets," *IEEE Trans. Veh. Technol.*, vol. 44, pp. 313–317, May 1995.

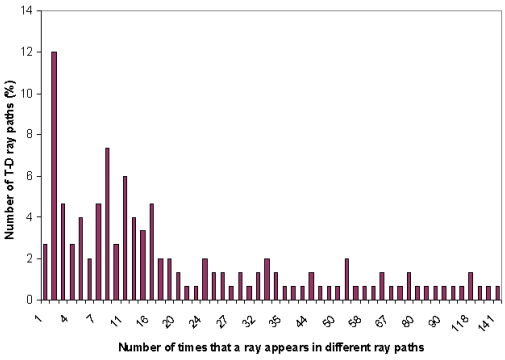

(a) $T - D$ class

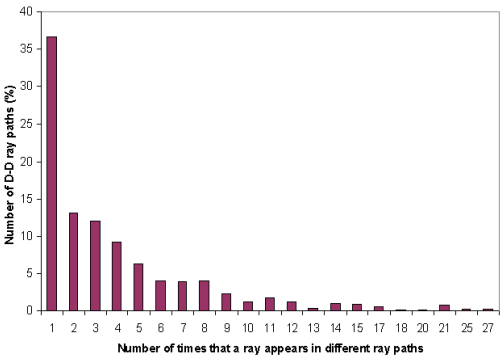

(b) $D - D$ class

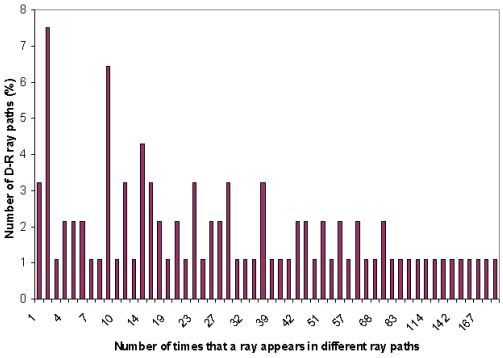

(c) $D - R$ class

Fig. 7. Number of times that rays belonging to the $T - D$, $D - D$ and $D - R$ classes, for a receiver at position (391 m, 100 m) of Fig. 5, are used.